PHYSICAL REVIEW B VOLUME 25, NUMBER 3 1 FEBRUARY 1982

Superconducting tunneling study of vanadium

J. Zasadzinski,* D. M. Burnell, and E. L. Wolf
Ames Laboratory—U.S. Department of Energy and Department of Physics, Iowa State University, Ames, Iowa 50011

G. B. Arnold
University of Notre Dame, Notre Dame, Indiana 46556

(Received 20 October 1980; revised manuscript received 3 August 1981)

The tunneling spectroscopy of McMillan and Rowell is extended to vanadium, with the use of clean and highly ordered structures of the form M-Al_2O_3-Al/V. The Eliashberg function $\alpha^2F(E)$ is determined and leads to $\lambda = 0.82 \pm 0.05$ and $\mu^*_{ph} = 0.15 \pm 0.03$. These tunneling results, the first available for V, indicate a smaller influence of paramagnon spin fluctuations in suppressing superconductivity in vanadium than recently suggested, but do not rule out such effects at a level $\lambda_s \sim 0.1$.

I. INTRODUCTION

The method of electron tunneling spectroscopy[1,2] provides a means of determining in detail the origin of superconductivity of a metal. Thus, one may obtain the effective phonon spectrum, $\alpha^2F(E)$, and Coulomb pseudopotential, μ^*, which give rise to the pair potential, $\Delta(E)$, and renormalization function, $Z(E)$, describing the superconducting state. This information permits calculation via the Eliashberg strong-coupling equations,[3] of the transition temperature T_c and other physical properties of the superconductor. In the case of the conventional metal-insulator-superconductor tunnel junction this analysis proceeds from the measured normalized tunneling conductance

$$\sigma(V) = \left(\frac{dI}{dV}\right)_S \Big/ \left(\frac{dI}{dV}\right)_N = \int_{-\infty}^{\infty} N_T(E) \frac{d}{dE} f(E + eV)\, dE \ , \quad (1)$$

where I and V are the tunneling current and bias voltage, respectively,

$$N_T(E) = \mathrm{Re}\{|E|/[E^2 - \Delta(E)^2]^{1/2}\} \ , \quad (2)$$

and $f(E)$ is the Fermi function

$$f(E) = [1 + \exp(E/kT)]^{-1} \ . \quad (3)$$

The analysis entails numerical inversion of the Eliashberg equations for the $\alpha^2F(E)$ and μ^* which generate the pair potential $\Delta(E)$ matching the data through relations (1) and (2).

The $3d$ transition element vanadium, superconducting $T_c = 5.4$ K,[4] appears to be the only naturally occurring elemental strong-coupling superconductor whose $\alpha^2F(E)$, Coulomb pseudopotential, μ^*, and pair potential, $\Delta(E)$, have not been determined using the standard tunneling methods. We emphasize that the inherent, if usually weak, energy dependence of the matrix elements α^2 makes the Eliashberg function $\alpha^2(E)F(E)$ a quantity distinct from the phonon density of states, $F(E)$, usually available from neutron scattering measurements.

There are several reasons for interest in a full tunneling spectroscopic study of vanadium. The most obvious is the desire to complete tabulation of the superconducting properties in the transition series.[5] The nuclear scattering properties of vanadium are such as to prohibit the usual detailed neutron scattering measurements of its lattice dynamics, although estimates of $F(E)$ are available from an inelastic incoherent neutron scattering technique.[6,7] From a basic point of view, the possible depression of the superconductivity of vanadium by fluctuations of $3d$ electrons into local ferro- or antiferromagnetic alignment (paramagnons) is of recent interest.[8,9] The participation of this element in the superconductivity of alloys (e.g., $V_{1-x}Ti_x$) and $A15$ compounds such as V_3Si and V_3Ga is a further reason for interest in its superconductive behavior.

The absence to date of a complete tunneling study for V is attributable to severe technical difficulties in making tunnel junctions with V in addition to the difficulty implied by the rather small size of the expected phonon structure in this case, $|\sigma/\sigma_{BCS} - 1| \leq 0.0025$.[2] (This is about $\frac{1}{20}$ of the magnitude of phonon structure in the case of lead.) The fabrication difficulties arise from the oxidation behavior of V, which forms several lower oxides of a metallic or semiconducting nature,[10] and from the rapid deterioration of the superconducting parameters of V with percent amounts of dissolved oxygen.[11]

Attempts to make tunneling junctions using barriers formed by thermally oxidizing V metal lead to

excessively large leakage currents. Vanadium tunnel junctions were fabricated by Noer[11] by evaporating V at room temperature onto prepared Al-Al_2O_3 electrode-barrier substrates, but these did not reveal phonon-induced structure in the measured conductance $\sigma(V)$. Improvement in this approach was reported by Robinson and Rowell[12] by cooling the Al-Al_2O_3 substrate to 4.2 K, but this did not yield an $\alpha^2F(E)$ function, possibly because of reaction of oxygen adsorbed on the Al_2O_3 with the first atomic layers of deposited V. Other aspects of the surface degradation problem in transition metal tunneling have been reviewed elsewhere.[13]

The present investigation has involved an ultrahigh vacuum method of fabricating proximity tunnel junctions of the form In-Al_2O_3–Al/V on carefully recrystallized V foil substrates. The remaining metallic Al layer acts to isolate the previously cleaned V surface from gaseous contaminants, leading to excellent tunneling spectra and essentially bulk superconducting properties for V. Since the experimental[14,15] and theoretical aspects[16,17] of the proximity electron tunneling spectroscopy (PETS) have been described elsewhere, these will not be repeated in any detail here. Because of the clean and highly ordered NS interfaces produced by the present techniques, complications recently noted in less ordered evaporated or quench-condensed structures do not appear.[18–20]

Briefly, a model of the NS sandwich is adopted in which the pair potential rises abruptly from a small value $\Delta_N(E)$ in the "normal" metal to $\Delta_S(E)$ at $x = d_N$, where the thickness d_N is assumed to be much less than the bulk coherence length. The N and S layers are assumed to be clean and in perfect electrical contact. The tunneling density of states presented by the N side of this structure has been calculated exactly[16] and forms the basis for our analysis. The physical features of $N_T(E)$ are revealed by its expansion, valid for energies $E \gg \Delta_S, \Delta_N$ (the phonon energy range). This is

$$N_T(E) = 1 + \frac{1}{2}\,\mathrm{Re}\frac{\Delta_N^2(E)}{E^2} + \frac{1}{2}\,\mathrm{Re}\frac{[\Delta_S(E)-\Delta_N(E)]^2}{E^2}\exp(2i\Delta K d_N) + \mathrm{Re}\frac{\Delta_N(E)[\Delta_S(E)-\Delta_N(E)]}{E^2}\exp(i\Delta K d_N)\ , \tag{4}$$

with

$$\Delta K d_N = \frac{2Z_N(E)\,d_N E}{V_{FN}} + i\frac{d_N}{l_n}\ . \tag{5}$$

Here $\Delta_S(E)$ is the value of the S pair potential at the NS interface. The N metal is described by the parameters d_N, $Z_n(E)$, and V_{FN} which are the film thickness, renormalization function, and Fermi velocity, respectively. In order to account for any scattering that might occur in the N layer or at the NS interface, a phenomenological scattering length parameter l_N has been included. As $\Delta K d_N \to 0$ the terms containing $\Delta_N(E)$ cancel and one obtains

$$N_T(E) = 1 + \frac{1}{2}\,\mathrm{Re}\frac{\Delta_S^2(E)}{E^2}\ , \tag{6}$$

which is the bulk S metal result as expected. If the properties of the N layer [$\Delta_N(E)$, $Z_n(E)$, d, and d/l] are *known,* then the data can be inverted to obtain the superconducting properties of the S metal by a method similar to that used originally by McMillan and Rowell.[2]

Because of the need to obtain the additional information regarding the N layer, a characterization of the superconducting substrate S basically requires two junctions of the form C-I-NS having *different* thicknesses, d_N, of the N layer, here Al. The first junction ideally has the minimum thickness d_N consistent with continuous coverage of the substrate S. With our ultrahigh vacuum methods and consequent atomically clean substrates this minimum d_N is in the range 20 to 30 Å. In order to determine the N-metal pair potential $\Delta_N(E)$, a second junction of larger d_N and consequent larger contributions to $N_T(E)$ in the phonon range of metal N must also be studied. The details of the procedures used to determine $\Delta_N(E)$ have been given in Ref. 17. It is important to realize that if the first junction has sufficiently small d_N, the influence of $\Delta_N(E)$ is small and in the nature of a correction. Thus the accuracy required in determination of $\Delta_N(E)$ need not be as great as in determining properties of S.

The objective of the present paper is to abstract from an extensive study of Al-V foil junctions[21] the information most pertinent to describe the superconducting properties of V. This is accomplished by describing in detail the analysis of a pair of typical junctions selected from a large set as best fulfilling the above requirements. A brief and preliminary account of portions of the present work has already been given.[22]

II. SAMPLES AND EXPERIMENTAL METHOD

Foils of zone-refined V (Ref. 23) were cut, electropolished and mounted in the ultrahigh vacuum chamber as described earlier.[14,15] Heating of the foil by passage of current at typically 3×10^{-9} Torr pro-

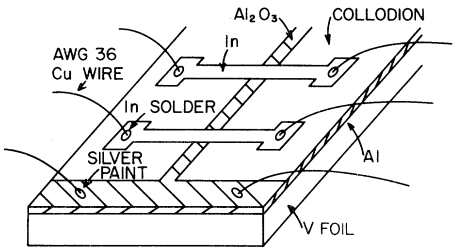

FIG. 1. Schematic drawing of tunnel junctions fabricated on a proximity sandwich. The substrate (not drawn to scale) is a 0.005-in.-thick foil of V, cleaned and recrystallized by resistive heating in ultrahigh vacuum. The shaded area depicts the thin Al layer (40 to 250 Å) which is deposited on the clean foil and is in good electrical contact with it. Exposure to laboratory air allows a thin layer of insulating Al_2O_3 to form and the junction area is defined by a collodion mask. Contact is made to the vapor-deposited In counterelectrode with In solder. Two contacts to the foil with silver paint allow a four-terminal measurement of each junction.

ceeded by stages to near the melting point, 1890 °C, releasing gaseous impurities and allowing recrystallization of the foil, producing a clean and highly ordered foil surface. As described previously[14,15] Al metal in stepped thicknesses ranging from 30 to 250 Å along the foil is deposited *in situ* at 10^{-9} Torr. This is done after the foil has been cooled to ~ -100 °C to promote smooth Al films; after returning to room temperature the vacuum system is vented to oxygen and then to atmosphere. Oxidation of the Al to form the tunneling barrier occurs during approximately an hour while all but a central strip and end of the foil are masked with collodion, prior to deposition at 10^{-6} Torr of thick (0.5–1 μm) In crossing counterelectrode strips. The sample configuration is sketched in Fig. 1. A total of 13 foils were processed, each resulting in up to ten tunnel junctions. Sample labeling is such that the fifth junction on the eighth processed foil of V is written as V-Al-8-5 or simply junction 8-5. The resistance ratio and transition temperature of the twelfth foil (from which junction 12-7 was obtained) were measured resistively as 14 and 5.35 ±0.03 K, respectively.

The choice of In as the counterelectrode allowed easy attachment of leads by soldering and permitted measurements at 1.37 K with the In electrode superconducting or driven normal with application of a 300-Oe magnetic field parallel to the foil. Tunneling measurements were made with the foil directly immersed in liquid He using standard techniques.[13]

III. MEASUREMENTS

Current-voltage plots obtained from several junctions, with both electrodes in the superconducting state, are shown in Fig. 2. The properties of the junctions are listed in Table I.

The I-V plot of junction 12-7, the sample from which the phonon spectrum of V is extracted, is shown in Fig. 3. The value of d_N, experimentally measured as 21 ±8 Å, is sufficiently small in this case that the gap region can be fit adequately with the usual BCS function, (2). Such a fit is shown in Fig. 4(a) (counterelectrode normal) at 1.37 K and 300 Oe, yielding a gap parameter $\Delta_0 = 0.80$ meV for V. A detailed fit of the normalized resistance with counterelectrode superconducting is shown in Fig. 4(b). This fit is obtained using the proximity density of states $N_T(E)$ (Ref. 16) with the same gap-edge value, $\Delta_0 = 0.80$ meV. The agreement of the gap-parameter values with and without the normalizing field demonstrates that the magnetic field employed to simplify the phonon spectra for the $\alpha^2F(E)$ analysis by removing the In contributions has an effect on the V parameters below the precision of our measurements. An independent estimate of this effect is made, following Meservey and Douglass,[24] in terms of their equation

$$\Delta(H)/\Delta(0) = 1 - D(H/H_c)^2 \ .$$

Here D is a function of the film thickness divided by the penetration depth, and is small compared with unity for thick films well below T_c, conditions which describe the V foils in question. Taking $H_c = 1420$ Oe for V (Ref. 4), one can estimate (at 300 Oe) from

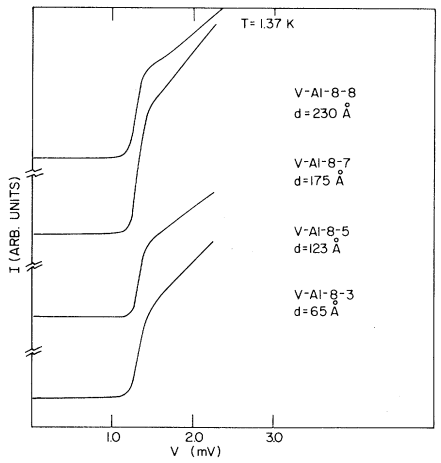

FIG. 2. Systematic study of I-V plots for tunnel junctions fabricated on the same V foil but with varying Al layer thicknesses. Leakage values for all junctions are below 1.5%. The In counterelectrode is superconducting and $\Delta_S + \Delta_{In}$ (location of peak in dI/dV) decreases from 1.32 meV for $d_{Al} = 65$ Å to 1.25 meV for $d_N = 230$ Å.

TABLE I. Characteristics of V proximity tunnel junctions selected for analysis.

Junction	Al layer thickness (Å)	Leakage %	Δ_{S0} (meV) [a]	Comments
V-Al-8-3	70	<1	0.78	Clear phonon structure of both V and Al. No discernible dip in the normalized conductance above Δ_{S0}.
V-Al-8-5	123	<1.5	0.75	Strong Al phonon structure; diminished V phonons; all exhibit a dip in the normalized conductance just above Δ_{S0}.
V-Al-8-7	175	<1.5	0.73	
V-Al-8-8	230	<1	0.71	
V-Al-12-7	21	2	0.80	Excellent V phonon structure, minimal Al interference. No dip in the normalized conductance near Δ_{S0}.

[a] Δ_{S0} determined by fitting the normalized conductance with the In normal to a thermally smeared BCS density of states at 1.37 K.

the discussion related to Fig. 11(c) of Ref. 24 that the fractional correction to Δ, namely $D(H/H_c)^2$ is of order 0.002. This is negligible in our measurements. A larger correction of the measured gap value, expected to be slightly reduced from the bulk value by the proximity layer, is described by[16]

$$\Delta_S = \Delta_S^{\text{bulk}}(1 - \pi R \Delta_S^{\text{bulk}}) \ ,$$

where $R = 2Z_N d_N/\hbar V_{FN}$.

Taking $R = 0.004\ (\text{meV})^{-1}$ as determined by $V_{FN} = 2.02 \times 10^8$ cm/sec for Al, $d_N = 21$ Å, and

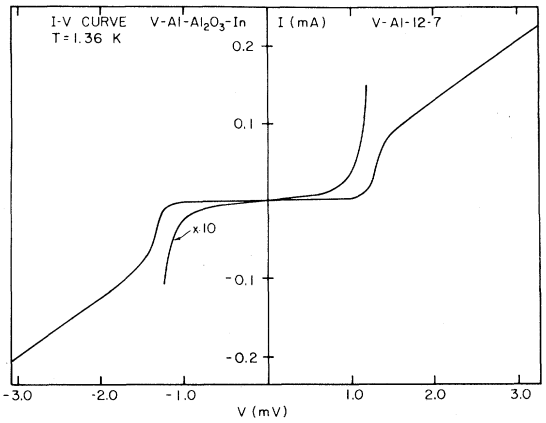

FIG. 3. Current-voltage plot for junction V-Al-12-7 which has a measured Al thickness $d_{Al} = 21 \pm 8$ Å. The In counterelectrode is superconducting and the ×10 trace indicates a leakage current less than 2% of that obtained with both electrodes normal. The steep rise at 1.33 meV corresponds to $\Delta_S + \Delta_{In}$ indicating (for $\Delta_{In} = 0.53$ meV) that $\Delta_S = 0.80$ meV for V.

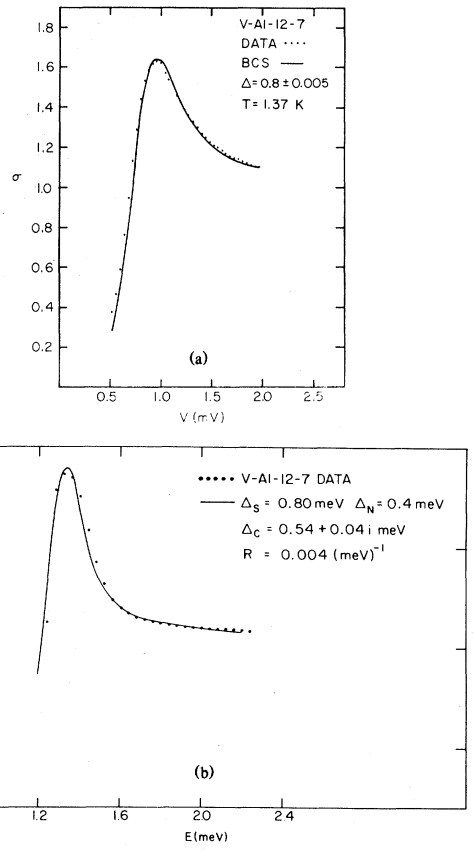

FIG. 4. (a) Comparison of measured normalized conductance for junction V-Al-12-7 to that of an ideal BCS superconductor with $\Delta = 0.80$ meV at 1.37 K. The measurements were done with an applied field of 300 Oe parallel to the foil to drive the In normal. (b) Comparison of measured normalized resistance data for V-Al-12-7 to the Arnold $N_T(E)$ at 1.37 K and $H = 0$. The In counterelectrode is described by $\Delta_c = 0.54 + i0.04$ meV which allows for a small amount of gap-edge broadening.

$Z_N = 1 + \lambda_N = 1.45$,[25] and $\Delta_S = 0.80$, this implies $\Delta_S^{\text{bulk}} = 0.81$ meV. This value agrees exactly with the 0.81 meV obtained by ultrasonic attenuation measurements[26] on V. It should be emphasized that the gap region displays none of the complicated structure associated with a barrier at the *NS* interface, indicating the assumption of a clean and sharp interface is justified. This may seem surprising at first when one considers the solubility of Al in V. However, the rate of interdiffusion of these metals at room temperature is extremely small.[27,28] Extrapolating the temperature-dependent diffusion constant to 300 K and using a characteristic handling time of 2 h, one obtains a reaction layer of <0.2 Å.

Figure 5 shows the first derivative dV/dI curves for junction 12-7, while in Fig. 6 the directly measured d^2V/dI^2 curves for 12-7(a) and 8-3(b) are compared. The latter junction, of $d_N = 70$ Å, shows a relatively stronger response at 36 meV, the energy of the prominent Al longitudinal phonon.[25,29] This second data set is used to determine the $\Delta_N(E)$ function required to make corrections in the first data set, for the small Al phonon contributions to $N_T(E)$. In Fig. 6 positive peaks in d^2V/dI^2 locate peaks in the phonon density of states of V or Al as marked. The energy scale in Fig. 6 has been corrected by subtracting the V gap energy $\Delta_0 = 0.8$ meV from the applied bias eV.

Quantitative analysis proceeds from the experimental BCS-reduced conductance $\sigma/\sigma_{\text{BCS}} - 1$ shown in Figs. 7(a) and 7(b) for vanadium junctions 12-7 and 8-3, respectively, hereafter referred to as 1 and 2.

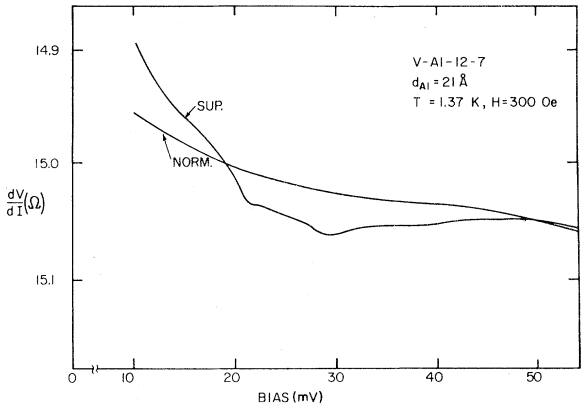

FIG. 5. Tracings of the dynamic resistance for junction V-Al-12-7 in the normal and superconducting state. An H field of 300 Oe was applied parallel to the foil plane to drive the In normal and remove the In phonon structure in the superconducting curve. Note the phonon structure near 10, 20, 30, and 40 meV for the superconducting curve. An H field of 5.5 kOe was applied perpendicular to the foil to obtain the normal curve.

One feature of the Al phonon responses in Fig. 7 which is notable is the apparently greater width of the 36-meV depression in thinnest Al film (1) compared to junction 2, for which $d_N = 70 \pm 8$ Å. In an analogous fashion, we will see below that the 36-meV feature in junction 2 is not as sharply defined as in *bulk* Al. This trend does not seem unreasonable in Al films of 20- and 70-Å thickness. However, it poses some difficulty in the correction procedure to be described.

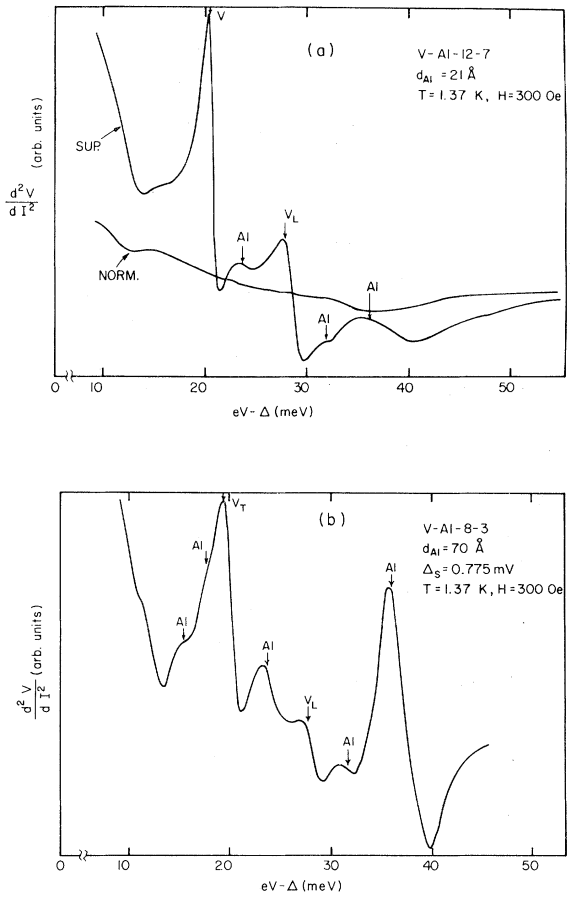

FIG. 6. (a) Tracing of directly measured d^2V/dI^2 vs energy for V-Al-12-7. The zero of energy is shifted to the gap edge to compare peaks in the data to peaks in the phonon spectrum of V and of Al which are marked by arrows. The second derivative is integrated to construct a dV/dI curve with clear phonon structure. (b) Tracing of d^2V/dI^2 data for V-Al-8-3 to indicate the change in tunneling characteristics as the Al layer thickness is increased. Here d_{Al} is measured to be 70 Å. The overall scale is reduced by approximately a factor of 2 compared to Fig. 6(a). Note the increase in relative amplitude of Al phonon structure to that of V as compared to Fig. 6(a).

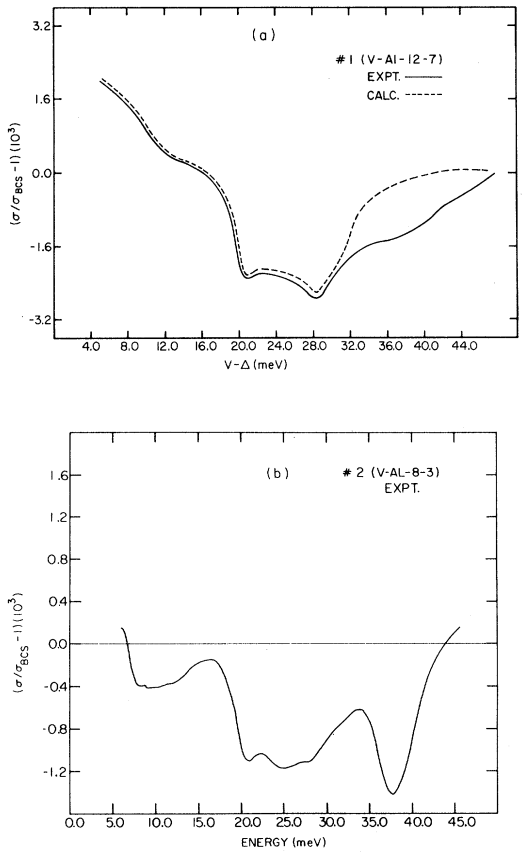

FIG. 7. (a) Reduced conductance for V-Al-12-7 from measured data (solid line) and calculated result of MMR inversion. The input parameters are $d_{Al}=20$ Å, $d/l=0.02$, and $\Delta_{S0}=0.80$ meV. The fit deviates beyond 30 meV because the initial approximation $\Delta_{Al}(E)=0$ does not account for Al phonon structure. (b) Reduced conductance for V-Al-8-3 using $\Delta_0=0.78$ meV.

IV. ANALYSIS OF DATA

The result of the first possible analysis for the phonon spectrum of V is indicated by the dashed line in Fig. 7(a). This calculated curve is obtained by setting the pair potential $\Delta_N(E)=0$ in Eq. (4), thus neglecting phonon structure from the Al, and using the McMillan stage III program[2,30] (MMR) as modified[17] to accept the exact proximity $N_T(E)$. The parameters $\lambda=0.62$, $\mu^*_{ph}=0.07$,[31,32] resulting from this inversion with $d=20$ Å and $d/l=0.02$, are of course only approximate by the neglect of Δ_N, which leads to the failure of the fit above 30 meV. We note, however, that the pair potential $\Delta^0_S(E)$ and renormalization function $Z^0_S(E)$ resulting from this inversion could be used as first approximations for V.

The next step is to provide as input to the exact $N_T(E)$ function[16] [approximated by Eq. (4)], a correcting $\Delta_N(E)$, to permit a more accurate $\Delta_S(E)$ to be determined by inversion of the data of sample 1. Two different pair-potential functions have been used for this purpose. The first, $\Delta_{N1}(E)$, is obtained from analysis of junction 2. A second, $\Delta_{N2}(E)$, for comparison, has been taken[21,33] from a previously published analysis of an Al/Nb junction having $d_N=27$ Å. Even though the differences between these two correcting functions are noticeable, we will demonstrate that the sensitivity of our determination of the desired properties of V to these differences is quite small.

The function $\Delta_{N1}(E)$ is obtained by initially determining from junction 2 the function $\Delta^0_{N1}(E)$ which is implied by data set 2 and the exact $N_T(E)$,[16] by using parameters d and d/l as appropriate, and on the assumption of input functions $\Delta^1_S(E)$, $Z^1_S(E)$, and $Z_N(E)$. The method used is described in Appendix A 2 of Ref. 17 and is similar to the method of Galkin *et al.*[34] The $Z_N(E)$ input was generated from a bulk Al $\alpha^2F(E)$ function[25] using the Eliashberg equations. The input $\Delta^1_S(E)$, $Z^1_S(E)$ functions were taken as the best available functions for V, in order to avoid an iterative sequence of inversions as described in Ref. 17. The functions used for this purpose were obtained by inversion of data set 1 using $\Delta_{N2}(E)$, $Z_{N2}(E)$.[21,33] We emphasize that this is merely a point of convenience and economy. Alternative choice here might have been Δ^0_S, Z^0_S described above or improved functions obtained by inverting data set 1 with Δ_N, Z_N calculated from the $\alpha^2F(E)_{Al}$ of Ref. 25. The $\Delta^0_{N1}(E)$ function thus obtained is defined only up to the end of data set 2, 45 meV, as shown in Fig. 7(b). In order to extend the energy range of the accurate determination of $\Delta_N(E)$, the corresponding $\alpha^2F(E)_{Al}$ [Fig. 8(a), solid curve] was determined, using a method described in the Appendix, and an extended $\Delta_{N1}(E)$ function [Fig. 8(b), solid curve] was finally obtained for use in correcting data set 1. Plots of derived $\Delta_{N1}(E)$ and $\alpha^2F(E)_{Al}$ functions are compared (dashed lines) in Fig. 8 with corresponding bulk functions following Ref. 25, which are seen to be generally similar. However, the $\alpha^2F(E)_{Al}$ function from junction 2 reveals a broadening and shift to lower energy of the longitudinal Al phonon peak near 36 mV. We do not find these minor differences to be suprising in a 70-Å film compared to bulk Al. In fact, the two $\alpha^2F(E)_{Al}$ functions agree rather well in inverse first moment, with $\lambda_{Al}=0.43$ from the bulk calculation versus $\lambda_{Al}=0.42$ from sample 2.

Vanadium properties are obtained by inversion of data set 1 using pair potentials $\Delta_{N1}(E)$ and $\Delta_{N2}(E)$ as the required input corrections. Results from the inversion using $\Delta_{N1}(E)$ and parameters $d=30$ Å, $d/l=0.14$ are shown in Fig. 9 [$\alpha^2F(E)_V$] and Fig. 10 (calculated conductance, dashed, compared to data,

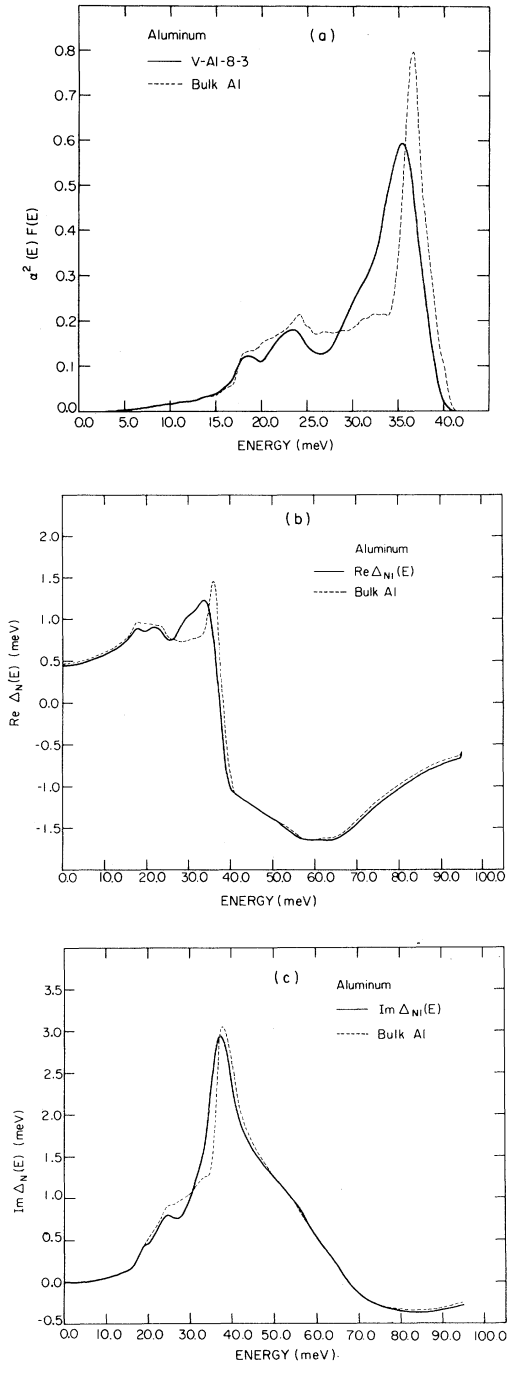

FIG. 8. (a) $\alpha^2F(E)_{Al}$ function deduced from sample 2 (solid curve) compared with function calculated for bulk Al in Ref. 2 (dashes). (b) Real part of pair potential $\Delta_{N1}(E)$ induced in 21-Å Al film of sample 1 by the thick vanadium substrate, assuming $\alpha^2F(E)_{Al}$ function (solid) for Al shown in (a). The pair potential calculated from the bulk Al (Dynes-Carbotte) $\alpha^2F(E)_{Al}$ is shown (dashed) for comparison. (c) Imaginary parts of the pair potentials shown in (b); solid curve derived from junction 2, dashed curve from bulk Al $\alpha^2F(E)$.

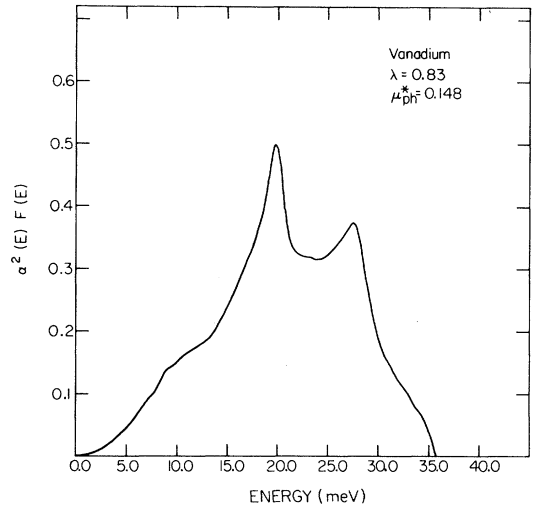

FIG. 9. Eliashberg function for V from sample 1, corresponding to $\lambda = 0.83$ and $\mu^*_{ph} = 0.148$.

solid). The d_N chosen is just at the upper end of the experimental range, in the interest of improving the fit in the 40-mV region. The superconducting parameters that result from this inversion are $\lambda = 0.83$, $\mu^*_{ph} = 0.15$, a calculated T_c (Refs. 31 and 32) of 6.2 K and $\omega_{log} = 14.8$ meV. For comparison, inversion of data set 1 using pair potential Δ_{N2} results in an extremely close fit (within 10^{-5}) to the measured conductance (taking $d_N = 20$ Å, $d/l = 0.14$) and parameters $\lambda = 0.79$, $\mu^*_{ph} = 0.14$, $T_c = 5.94$ K. The corre-

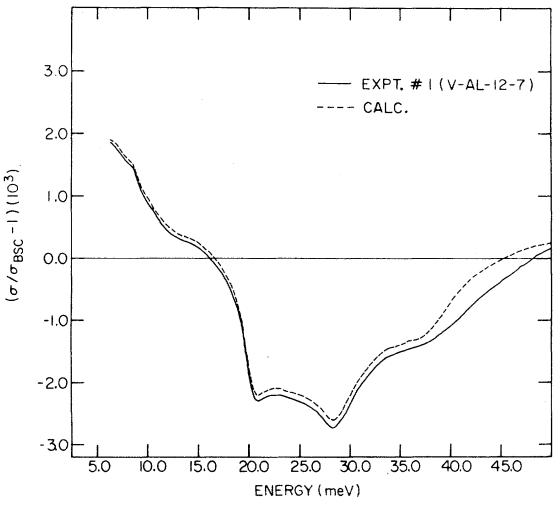

FIG. 10. Comparison of reduced conductance for sample 1 (solid curve) with calculation (dashed curve) using correction $\Delta_{N1}(E)$ corresponding to the $\alpha^2F(E)_V$ function of Fig. 9.

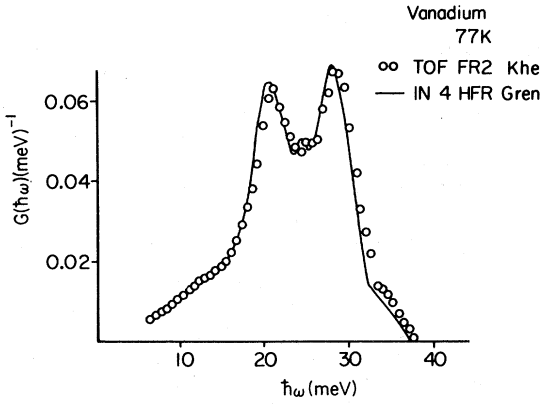

FIG. 11. Phonon spectrum $F(E)$ for vanadium at 77 K determined by incoherent inelastic neutron scattering. After Ref. 6 with permission of the author.

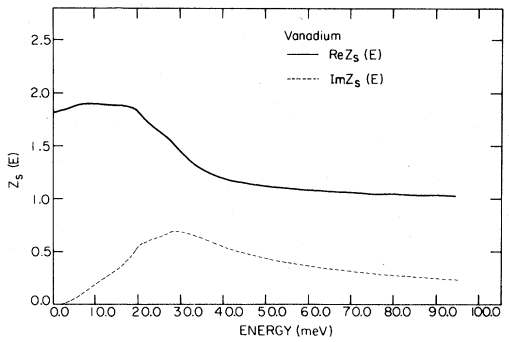

FIG. 13. Renormalization function $Z_S(E)$ for vanadium in the superconducting state. Real part (solid curve) and imaginary part (dashed curve) are shown.

sponding $\alpha^2F(E)_V$ function (not shown) is extremely close to one published earlier.[22] The present $\alpha^2F(E)_V$ function gives a slight increase in the longitudinal peak (0.375 vs 0.36) and improved accuracy near the cutoff energy, here (Fig. 9) determined as 35.7 meV.

In both cases the calculated T_c values from the Allen-Dynes formula[21] are higher than the measured 5.35 K; however, the difference is within our estimates of uncertainty in λ and μ^* using an analysis of error propagation in this formula.[17] While we prefer the present $\alpha^2F(E)_V$ function (Fig. 9), the rather small differences in the resulting parameters λ and μ^* are taken as a measure of the overall uncertainty in our determination. For comparison with the $\alpha^2F(E)_V$ we have reproduced in Fig. 11 the $F(E)_V$ obtained by neutron scattering,[6] which is also close to the $F(E)_V$ of Ref. 7. Figures 12 and 13, respectively, show the pair potential $\Delta_S(E)$ and superconducting renormalization function $Z_S(E)$ for V, corresponding to the $\alpha^2F(E)_V$ of Fig. 9. Any differences between these functions and those generated using $\Delta_{N2}(E)$ are extremely small.

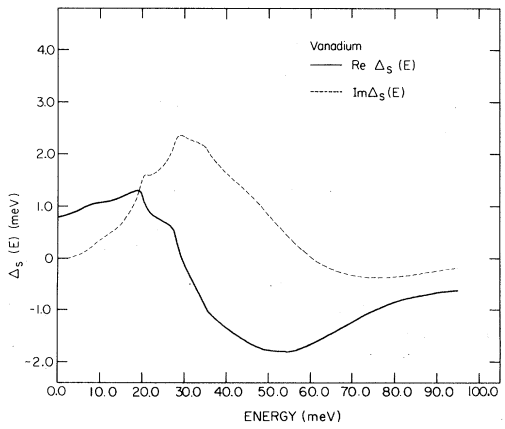

FIG. 12. Pair potential $\Delta(E)$ for vanadium; real part (solid curve) and imaginary part (dashed curve).

V. DISCUSSION

The $\alpha^2F(E)_V$ function obtained is the first available for V, a material of considerable current interest. The treatment of the data has included corrections for the induced Al pair potential in the proximity junction.

A. Correction procedures

Two rather different correction functions have been used. Pair potential $\Delta_{N1}(E)$, derived from junction 2, is quite similar [see Fig. 7(b)] to the $\Delta_N(E)$ implied by the bulk Al calculation.[25] Applied to the $N_T(E)$ of junction 1, it provides a correction, to within 0.02% of experiment up to about 39 meV (dashed curve, Fig. 10). Note that this range includes the peak in $\alpha^2F(E)_{Al}$. However, it fails, beyond 40 meV, to fully correct the conductance, which we take as a consequence of the greater width of the Al features in the thin 21-Å film of junction 1. This fit leads to $\lambda=0.83$, $\mu^*_{ph}=0.15$, and $T_c=6.2$ K. The correcting pair potential $\Delta_{N2}(E)$ (not shown) provides a better correction beyond 39 meV: in fact, the calculated conductance obtained using this function cannot be distinguished from the experimental curve on the scale of Fig. 10, over the whole energy range.[21] This function (which closely resembles the

dotted curves in Figs. 9 and 10 of Ref. 17) differs from $\Delta_{N1}(E)$ in having a stronger variation in the range 40 to 45 meV and a greater broadening of its features. The broadening we believe is associated with the origin of this function from a thinner Al film, $d_N = 27$ Å, similar to the present junction 1. The Δ_{N2} function, which is regarded as a stronger correction, leads to $\lambda = 0.79$ and $\mu^*_{ph} = 0.15$. Because we are concerned with a correction, the parameter λ deduced for V differs by not more than 5% between the two cases, which we accept as an estimate of the uncertainty in our determination. In summary, our result is $\lambda = 0.82 \pm 0.05$ and $\mu^*_{ph} = 0.15 \pm 0.03$ for V. We know of no other direct experimental determination with which to compare these values.

B. Properties of vanadium

The moments of the $\alpha^2F(E)$ function are conventionally defined using the relations

$$\langle f(E) \rangle = \frac{2}{\lambda} \int_0^{E_0} f(E) \frac{\alpha^2F(E)}{E} dE \ ,$$

where

$$\lambda = 2 \int_0^{E_0} \alpha^2 \frac{F(E)}{E} dE \ ,$$

and E_0 is the maximum phonon energy. For vanadium we find from the $\alpha^2F(E)_V$ function of Fig. 9 the values

$$\langle E \rangle = 17.1 \text{ meV}, \quad \langle E^2 \rangle = (18.76 \text{ meV})^2$$

and $E_{log} = 14.8$ meV, where $E_{log} \equiv \exp\langle \ln E \rangle$. The peak positions at 19.8 and 27.4 meV may be compared with 20.3 and 28.3 meV in the neutron data of Fig. 11. The $\alpha^2F(E)$ function has a shape generally similar to that we previously have obtained for Nb in that the high-energy longitudinal peak is smaller than the transverse peak. As in the case of Nb, this relative weighting differs from that observed in $F(E)$, the neutron scattering phonon spectrum in Fig. 11. In principle, this difference may be attributed to $\alpha^2(E)$ being a decreasing function of energy. An indication that this is not entirely the correct explanation, at least in Nb, has been given by Butler *et al.*[35] in a calculation making use of measured neutron scattering line widths in Nb and giving a very strong longitudinal peak. As has been mentioned elsewhere,[17,36] it is possible that the relative reduction of the longitudinal peak may arise, in part for the local nature of the tunneling measurement and impurities, or other disorder in the surface or interfacial region of the V. On the other hand, recent proximity tunneling studies of Ta reveal a considerably stronger longitudinal peak,[37] closer in its relationship to the transverse peak than to that observed in neutron scattering. The fact that the Ta and V foils are processed in an equivalent fashion makes clear that the proximity method itself is not the origin of the reduced longitudinal peak and indicates that the difference originates in the metal foils, in either the degree of surface cleanliness achieved or in some property of the coupled electron-phonon system.

The parameters $\lambda = 0.82 \pm 0.05$ and $\mu^*_{ph} = 0.15 \pm 0.03$, which we quote for V (using the conventional Eliashberg equations with no paramagnon term), are both somewhat larger than one would expect for a typical superconductor of $T_c = 5.4$ K and $E_{log} = 14.8$ meV. Following the empirical relation of T_c/E_{log} vs λ demonstrated in Fig. 10 of Allen and Dynes,[31] the expected λ for V would be about 0.69. The range of values tabulated for μ^*_{ph} in Ref. 31 is centered close to 0.1 and includes none larger than 0.12. On the other hand, our values are much smaller than those of Ref. 8: $\lambda_{ph} = 1.04$ and $\mu^* = 0.55$. The μ^* of Ref. 8 is obtained by solving the Eliashberg equations with no paramagnon term for $T_c = 5.4$ K using a calculated $\alpha^2F(E)_V$ corresponding to $\lambda = 1.04$. This indirectly obtained value for λ is beyond the range of uncertainty in our determination. In our work we have deduced λ and μ^* from the tunneling measurements alone (no use is made of the experimental T_c) and then have *calculated* T_c to be 15% higher than the experimental using the Dynes-Allen expression.[31] In a further check the T_c was calculated[38] on the basis of our $\alpha^2F(E)_V$ and μ^*_{ph} values using the Eliashberg equations (with no paramagnon term) giving 6.4 K, in substantial agreement with the Dynes-Allen formula. We cannot rule out the possibility that this inconsistency in the calculated T_c (and the slightly increased values of λ and μ^*) are consequences of weak paramagnon effects in V which are not dealt with in our analysis. However, we believe, on the basis of the present results, that a value of the parameter λ_s, as defined in Ref. 8, much larger than 0.1 is unlikely.

ACKNOWLEDGMENTS

We gratefully acknowledge the donation of vacuum chamber by Bell Laboratories courtesy of Dr. J. M. Rowell, and receipt of a Cottrell grant from the Research Corporation. For technical assistance we thank Harlan Baker, Dr. A. Bevolo, and Duke Sevde. The collaboration of W. Kent Schubert in portions of this work is gratefully acknowledged. We thank Professor J. P. Carbotte for calculated values of $\alpha^2F(E)$ for Al and Dr. P. Schweiss for permission to reproduce Fig. 11. Ames Laboratory is operated for the U.S. Department of Energy by Iowa State University under Contract No. W-7405-Eng-82. This research was supported by the Director for Energy Research, Office of Basic Energy Sciences, WPAS-KC-02-02-02, and by NSF Grant No. DMR 80-19739.

APPENDIX: DETERMINATION OF $\alpha^2F(E)_{Al}$

In this Appendix we shall describe the means by which $\alpha^2F(E)_{Al}$ was found. In PETS II (Ref. 17) we have already discussed the technique by which $\Delta_{Al}(E)$ may be determined. A disadvantage of the approach described there is that in order to find the aluminum pair potential for a given energy range, one requires conductance data over a *larger* energy range. This necessity is an unfortunate aspect of the Kramers-Kronig analysis which must be employed in the determination (see PETS II for details).

Typically, conductance data for these studies did not extend further than 50 mV or so. By employing numerically generated test data for the conductance between 0 and 50 mV, we have observed that the error in the $\Delta_{Al}(E)$ determination increases from between 1 and 2% up to 40 mV to 14% at 50 mV, with steadily increasing error in between. Thus, the program which determines $\Delta_{Al}(E)$ is acceptably accurate up to 40 mV when the conductance data extend to 50 mV. Since 40 mV is just above the cutoff in $\alpha^2F(E)_{Al}$ this suggests an alternative scheme for generating $\Delta_{Al}(E)$ at *all* energies.

Since $\Delta_{Al}(E)$ is accurately determined for energies up to 40 mV, one may obtain the pairing self-energy $\phi_{Al}(E)$ if $Z_{Al}(E)$ is assumed to be known:

$$\phi_{Al}(E) = Z_{Al}(E)\Delta_{Al}(E) \ .$$

We initially chose $Z_{Al}(E)$ to be equal to its proximity-effect induced value obtained via the Dynes-Carbotte $\alpha^2F(E)_{Al}$ function [see Eq. (6), PETS II]. From equation (5) of PETS II, we have

$$\mathrm{Im}\phi_{Al}(E) = \pi \int_{\Delta_{S0}}^{E} dE' \mathrm{Re}\left[\frac{\Delta_S}{\Omega_S'}\right] \alpha^2F(E-E')_{Al} \ .$$

This relation is readily inverted numerically to find $\alpha^2F(E)_{Al}$, since $\Delta_S' = \Delta_S(E')$ and $\Omega_S' = [(E')^2 - \Delta_S(E')]^{1/2}$ are known.

Clearly, in order to find $\alpha^2F(E)_{Al}$, all one requires is knowledge of $\mathrm{Im}[Z_{Al}(E)\Delta_{Al}(E)]$ for energies up to the cutoff energy for the phonon spectrum in Al. Since $Z_{Al}(E)$ is assumed known and $\Delta_{Al}(E)$ is accurately determined up to this energy, $\alpha^2F(E)_{Al}$ can be obtained. From this calculation one may now insert $\alpha^2F(E)_{Al}$ into Eqs. (5) and (6) in order to find $\Delta_{Al}(E)$ and $Z_{Al}(E)$ at *any* energies (taking $\mu_{Al}^* = 0.11$). In principle, the consistency of the initial assumption for $Z_{Al}(E)$ may then be checked by taking the new $Z_{Al}(E)$ and iterating the above procedure to obtain an improved $\alpha^2F(E)_{Al}$; but, in practice, this is not necessary.

An important feature of our technique for obtaining $\Delta_{Al}(E)$ and $\alpha^2F(E)_{Al}$ is its lack of dependence on μ_{Al}^*. In fact, the value of μ_{Al}^* has an influence on our results only for the calculated values of $\mathrm{Re}[\Delta_{Al}(E)]$. As emphasized in the text, $\Delta_{Al}(E)$ induces a small correction to the calculated Vanadium properties. Small variations in μ_{Al}^* should accordingly have little effect.

---

*Present address: Solid State Sciences Division, Argonne National Laboratory, Argonne, Ill. 60439.

[1]Ivar Giaever, Phys. Rev. Lett. 5, 147 (1960).
[2]W. L. McMillan and J. M. Rowell, in *Superconductivity,* edited by R. D. Parks (Dekker, New York, 1969), p. 561.
[3]G. M. Eliashberg, Zh. Eksp. Teor. Fiz. 38, 966 (1960) [Sov. Phys. JETP 11, 696 (1969)].
[4]R. Radebaugh and P. H. Keesom, Phys. Rev. 149, 209 (1966).
[5]W. H. Butler, Phys. Rev. B 15, 5267 (1977).
[6]P. Schweiss, Report No. KFK 2054 (unpublished).
[7]G. F. Syrykh, A. P. Zhernov, M. G. Zemlyanov, S. P. Mironov, N. A. Chernoplekov, and Y. L. Shitikov, Zh. Eksp. Teor. Fiz. 70, 353 (1976) [Sov. Phys. JETP 43, 183 (1976)].
[8]H. Rietschel and H. Winter, Phys. Rev. Lett. 43, 1256 (1979).
[9]J. M. Daams, B. Mitrović, and J. P. Carbotte, Phys. Rev. Lett. 46, 65 (1981).
[10]J. B. Goodenough, in *Progress in Solid State Chemistry,* edited by H. Reiss (Pergamon, Oxford, 1971), Vol. 5, p. 145.
[11]R. J. Noer, Phys. Rev. B 12, 4882 (1975).
[12]B. Robinson and J. M. Rowell, in *Transition Metals—1977,* edited by M. J. G. Lee, J. M. Perz, and E. Fawcett, IOP Conf. Ser. No. 39 (IOP, Bristol and London, 1978), p. 666.
[13]E. L. Wolf, Rep. Prog. Phys. 41, 1439 (1978); E. L. Wolf, J. Zasadzinski, G. B. Arnold, D. F. Moore, J. M. Rowell, and M. R. Beasley, Phys. Rev. B 22, 1214 (1980).
[14]E. L. Wolf and J. Zasadzinski, Phys. Lett. 62A, 165 (1977); Ref. 12.
[15]E. L. Wolf, J. Zasadzinski, J. W. Osmun, and G. B. Arnold, Solid State Commun. 31, 321 (1979); J. Low Temp Phys. 40, 19 (1980); Z. G. Khim, D. Burnell, and E. L. Wolf, Solid State Commun. 39, 159 (1981).
[16]G. B. Arnold, Phys. Rev. B 18, 1076 (1978).
[17]G. B. Arnold, J. Zasadzinski, J. W. Osmun, and E. L. Wolf, J. Low Temp. Phys. 40, 227 (1980).
[18]S. Bermon and C. K. So, Phys. Rev. B 17, 4256 (1978).
[19]Z. G. Khim and W. J. Tomasch, Phys. Rev. Lett. 42, 1227 (1979).
[20]Z. Ovadyahu and O. Entin-Wohlman, J. Phys. F 9, 2091 (1979).
[21]John F. Zasadzinski, thesis (Iowa State University, 1979) (unpublished).
[22]J. Zasadzinski, W. K. Schubert, E. L. Wolf, and G. B. Arnold, in *Proceedings of the Third International Conference on Superconductivity of d- and f-Band Metals,* edited by H. Suhl and M. B. Maple (Academic, New York, 1980), p. 159.
[23]MRC Corp. MARZ grade material.
[24]R. Meservey and D. H. Douglass, Jr., Phys. Rev. 135, A24 (1964).

[25]H. K. Leung, J. P. Carbotte, D. W. Taylor, and C. R. Leavens, Can. J. Phys. 54, 1585 (1976). We thank Professor Carbotte for providing punched output of the $\alpha^2F(E)$ function.

[26]J. L. Brewster, M. Levy, and I. Rudnick, Phys. Rev. 132, 1062 (1963).

[27]S. P. Murarka, M. S. Anand, and R. P. Agarwala, Acta. Metall. 16, 69 (1968).

[28]K. Nakamura, S. S. Lau, M-A. Nicolet, and J. W. Mayer, Appl Phys. Lett. 28, 277 (1976).

[29]P. M. Chaikin, G. Arnold, and P. K. Hansma, J. Low Temp. Phys. 26, 229 (1963).

[30]W. N. Hubin, Tech. Report No. 182, ARPA SD-B1, University of Illinois (unpublished).

[31]P. B. Allen and R. C. Dynes, Phys. Rev. B 12, 905 (1975).

[32]Following the recommendation of Ref. 31 we have corrected the μ^* value from that determined by the cutoff energy in the inversion program using the relation $(\mu^*_{ph})^{-1} = (\mu^*_{co})^{-1} + \ln(\omega_C/\omega_D)$, where ω_C and ω_D are the cutoff energy and the highest energy in the phonon spectrum, respectively. Values of μ^* quoted in this paper are understood to be μ^*_{ph} values.

[33]The $\Delta_{N2}(E)$ function used is quite similar to that shown (dotted line) in Figs. 9 and 10 of Ref. 17, with scaling corrections to account for the substitution of V for Nb as the *S*-layer inducing superconductivity.

[34]A. A. Galkin, A. I. D'yachenko, and V. M. Svistunov, Zh. Eksp. Teor. Fiz. 66, 2262 (1974) [Sov. Phys. JETP 39, 1115 (1974)].

[35]W. H. Butler, H. G. Smith, and N. Wakabayashi, Phys. Rev. Lett. 39, 1004 (1977).

[36]G. B. Arnold and E. L. Wolf (unpublished).

[37]E. L. Wolf, R. J. Noer, D. Burnell, Z. G. Khim, and G. B. Arnold, J. Phys. F 11, L23 (1981); and unpublished data.

[38]We are indebted to Dr. William H. Butler for carrying out this calculation, using methods described by W. H. Butler, Phys. Rev. Lett. 44, 1516 (1980).